VIII International Conference on Fracture Mechanics of Concrete and Concrete Structures
FraMCoS-8
J.G.M. Van Mier, G. Ruiz, C. Andrade, R.C. Yu and X.X. Zhang (Eds)

A COUPLED INTERFACE-BODY NONLOCAL DAMAGE MODEL FOR THE ANALYSIS OF FRP STRENGTHENING DETACHMENT

S. MARFIA[*], E. SACCO[*] AND J. TOTI[*]

[*] Università di Cassino e del Lazio Meridionale, Department of Civil and Mechanical Engineering
Università di Cassino e del Lazio Meridionale (DiCeM)
Via Marconi, 03043 Cassino, Italy
e-mail: marfia@unicas.it, www.unicas.it
e-mail: sacco@unicas.it, www.unicas.it
e-mail: jessica.toti@unicas.it, www.unicas.it

Key words: Interface-body damage, Detachment phenomenon, Nonlocal model

Abstract: In the present work, a new model of the FRP-concrete or masonry interface, which accounts for the coupling occurring between the degradation of the cohesive material and the FRP-body interface, is presented. A nonlocal damage and plasticity model is developed for the quasi-brittle material; a model which accounts for damage, unilateral contact and friction effects is developed for the interface. Two different ways of performing the coupling between the body damage and the interface damage are proposed and compared. Some numerical applications are carried out in order to assess the performances of the proposed model in reproducing the mechanical behavior of the masonry material strengthened with external FRP reinforcements.

1 INTRODUCTION

The use of Fiber Reinforced Plastic (FRP) materials for the strengthening of existing concrete and masonry elements is growing; recently, many structures have been reinforced adopting FRP and several experimental and modeling scientific works have been developed [1]-[5]. The use of FRP materials applied on the external surface of concrete or masonry structures created new modeling problems. One of the main problems in the use of FRP is the so-called detachment phenomenon, which consists in the sudden detachment of the FRP reinforcement from the concrete or masonry surface.

In particular, the collapse for loss of cohesion in the composite structures is generally caused by the evolution of different phenomena of damage in a narrow region near the interface.

The concrete as well as the masonry are quasi-brittle materials, which exhibit a mechanical response characterized by damage with softening due to the development of microcracks. Thus, two damage effects could be presented in the quasi-brittle reinforced structural elements: the body damage, which develops inside the domain of the strengthened element, and the interface damage, which occurs at the FRP-concrete or masonry interface. Experimental evidences demonstrate that the detachment of the FRP from the support material occurs often with peeling of a thin layer from the external surface of the quasi-brittle material; this collapse behavior is due to the fact that the strength of the glue used to apply the FRP to the support is generally greater than the strength of the concrete or masonry support. Thus, the damage of the support material influences the detachment of the FRP. From this observation, it can be deduced that the body damage and the interface damage cannot evolve independently one from the other; in other words, they are coupled [6].

In the present work, a new model of the FRP-concrete or masonry interface, that takes

into account the coupling occurring between the degradation of the cohesive material and the FRP detachment, is presented. A new nonlocal damage and plasticity model is developed for the quasi-brittle material. An interface model which accounts for damage, unilateral contact and friction effects is developed. Two different ways of performing the coupling between the body and the interface damage are proposed. Both the approaches assume that the interface damage is influenced not only by the detachment stresses but also by the body damage computed on the bond surface. The first approach ensures that the interface damage is not lower than the body damage evaluated at the bond surface [7]. The second approach is based on micromechanical considerations. Some numerical applications are performed in order to assess the performances of the proposed coupled interface models in reproducing the mechanical behavior of the masonry material strengthened with external FRP reinforcements.

2 A COUPLED BODY-INTERFACE DAMAGE MODEL

The structural system, schematizing the FRP reinforced concrete or masonry element, is studied in the framework of small strain and displacement regime. The system, consists in three subsystems: the body Ω_1, modeling the concrete or masonry element, characterized by a cohesive constitutive law; the body Ω_2, modeling the FRP strengthening, characterized by a linear elastic behavior; the interface $\Im$, modeling the bond between the reinforcement and the quasi-brittle material, characterized by a damaging behavior with friction and unilateral contact effects.

It can be remarked that the interface $\Im$ is assumed to be constituted by three layers: the glue, whose mechanical properties are generally much better than those of the support cohesive material; a thin layer of the support cohesive material in which, during the application of the reinforcement, the glue penetrates, improving its mechanical properties and a further thin layer of the support cohesive material in which the detachment process occurs.

Indeed, the first two layers remain joined to the FRP strengthening after the complete detachment. The interface damaging process, occurring in the third layer, can be due to the stresses induced by the detachment action and also by the degradation of the support material . As a consequence, the damage occurring in the body Ω_1 influences the behavior and the detachment process of the interface; on the contrary, it can be assumed that the damage of the third layer, generated by the detachment stresses, remains localized in the interface, i.e. it does not influences the body damage.

In order to take into account these two possible damaging effects, an interface coupled damage model should be adopted. In fact, the coupling ensures that the damage evolution at the interface depends on the body damage and not vice-versa.

The constitutive laws of the body Ω_1, of the interface $\Im$, neglecting the coupling between the body and the interface damage, and of interface $\Im$, considering two different ways of coupling the body and interface degradation, are presented in the following.

2.1 Body nonlocal damage model for the cohesive material

A plastic nonlocal damage model, characterized by the following constitutive law, is considered for the body Ω_1:

$$\begin{aligned}\boldsymbol{\sigma}^{\Omega} = \bar{\boldsymbol{\sigma}}^{\Omega}\,[&(1-D_t^{\Omega})H(\mathrm{sgn}(tr(\mathbf{e}^{\Omega}))+\\ &+(1-D_c^{\Omega})(1-H(\mathrm{sgn}(tr(\mathbf{e}^{\Omega}))))]\end{aligned} \tag{1}$$

with $\boldsymbol{\sigma}^{\Omega}$ the stress tensor, D_t^{Ω} and D_c^{Ω} the damage variables in tension and in compression, respectively, the symbol $\mathrm{sgn}(\bullet)$ indicating the sign of the variable $\bullet$, $H(\bullet)$ the Heaviside function (i.e. $H(\bullet)=1$ if $\bullet \geq 0$, otherwise $H(\bullet)=0$) and $\bar{\boldsymbol{\sigma}}^{\Omega}$ the effective stress tensor defined as:

$$\bar{\boldsymbol{\sigma}}^{\Omega} = \mathbf{C}^{\Omega}\left(\boldsymbol{\varepsilon}^{\Omega} - \boldsymbol{\varepsilon}_p^{\Omega}\right) = \mathbf{C}^{\Omega}\mathbf{e}^{\Omega} \tag{2}$$

where $\mathbf{C}^{\Omega}$ is the elastic tensor, $\boldsymbol{\varepsilon}^{\Omega}$, $\boldsymbol{\varepsilon}_p^{\Omega}$ and $\mathbf{e}^{\Omega}$ are the total strain, the plastic strain and the elastic strain tensors, respectively. The following plastic yield function is introduced:

$$f = A-\left(\bar{\sigma}_1-\sigma_y\right)\left(\bar{\sigma}_2-\sigma_y\right)+ \\ +B\left(\left\langle\bar{\sigma}_1-\sigma_y\right\rangle_-^2+\left\langle\bar{\sigma}_2-\sigma_y\right\rangle_-^2\right) \quad (3)$$

with $\bar{\sigma}_1$ and $\bar{\sigma}_2$ the principal stresses of the effective stress tensor, σ_y the yield stress and A and B two parameters governing the shape of the yield function, which represents a brunch of a modified hyperbola. The evolution law for the plastic strain is set as:

$$\dot{\boldsymbol{\varepsilon}}_p^{\Omega}=\dot{\xi}\frac{\partial f}{\partial\bar{\boldsymbol{\sigma}}^{\Omega}} \qquad \kappa^{\Omega}=\int_0^t\left\|\dot{\varepsilon}_p^{\Omega}\right\|dt \quad (4)$$

with κ^{Ω} the accumulated plastic strain. The model is completed with the classical loading-unloading Khun-Tucker conditions, $\dot{\xi}\geq 0,\quad f\leq 0,\quad \dot{\xi}f=0$.

As the softening constitutive law is introduced, localization of the strain and damage could occur. In order to overcome this pathological problem, to account for the correct size of the localization zone and, also, to avoid strong mesh sensitivity in finite element analyses, a nonlocal constitutive law is considered. In particular, an integral nonlocal model is adopted for the damage in compression and in tension.

The evolution of the compressive damage variable is governed by the following law:

$$\tilde{D}_c^{\Omega}=\max_{history}\left\{\min\left\{1,\tilde{D}_c^{\Omega}\right\}\right\} \quad (5)$$

with

$$D_c^{\Omega}=-\frac{2}{\kappa_u^3}\left(\bar{\kappa}^{\Omega}\right)^3+\frac{3}{\kappa_u^2}\left(\bar{\kappa}^{\Omega}\right)^2 \quad (6)$$

with κ_u is the final accumulated plastic strain associated with the compressive damage $D_c^{\Omega}=1$ and $\bar{\kappa}^{\Omega}$ the nonlocal accumulated plastic strain, evaluated at the point $\mathbf{x}$, as:

$$\bar{\kappa}^{\Omega}\left(\mathbf{x}\right)=\frac{1}{\Omega_r}\int_{\Omega}\psi\left(\mathbf{x},\mathbf{y}\right)\kappa^{\Omega}\left(\mathbf{y}\right)d\Omega \quad (7)$$

where $\mathbf{y}$ is a typical point of the body Ω_1, $\Omega_r=\int_{\Omega}\psi\left(\mathbf{x},\mathbf{y}\right)d\Omega$ is the normalized volume, $\psi\left(\mathbf{x}\right)=\left\langle 1-\left\|\mathbf{x}-\mathbf{y}\right\|^2/R^2\right\rangle_+$ is the weight function with R the radius of the nonlocal integration domain and the symbol $\left\langle\bullet\right\rangle_+$ denoting the positive part of the number $\bullet$.

The evolution of the tensile damage parameter is governed by an exponential law, set as:

$$D_t^{\Omega}=\max_{history}\left\{\min\left\{1,\tilde{D}_t^{\Omega}\right\}\right\} \quad (8)$$

with

$$\tilde{D}_t^{\Omega}=\frac{\bar{\varepsilon}_{eq}^{\Omega}-\varepsilon_0\exp\left(-k\left(\bar{\varepsilon}_{eq}^{\Omega}-\varepsilon_0\right)\right)}{\bar{\varepsilon}_{eq}^{\Omega}} \quad (9)$$

$\bar{\varepsilon}_{eq}^{\Omega}\left(\mathbf{x}\right)$ is the equivalent nonlocal strain, evaluated at the point $\mathbf{x}$ as:

$$\bar{\varepsilon}_{eq}^{\Omega}\left(\mathbf{x}\right)=\frac{1}{\Omega_r}\int_{\Omega_1}\psi\left(\mathbf{x},\mathbf{y}\right)\varepsilon_{eq}^{\Omega}\left(\mathbf{y}\right)d\Omega \quad (10)$$

$\varepsilon_{eq}^{\Omega}=\sqrt{\left\langle\varepsilon_1\right\rangle_+^{\,2}+\left\langle\varepsilon_2\right\rangle_+^{\,2}}$ is the equivalent strain, where ε_1 and ε_2 are the local principal strains [8].

Moreover the condition $D_t^{\Omega}\geq D_c^{\Omega}$ is introduced, in order to prescribe that the damage in tension is not lower than the damage in compression.

2.2 Interface damage model without coupling

A phenomenological interface model based on the micromechanical idea, developed in [9] and [10], is proposed. The displacement fields of the two joined bodies are denoted as $\mathbf{u}^1$ and $\mathbf{u}^2$, while the relative displacement at the typical point $\mathbf{x}^{\Im}$ of the interface $\Im$ is defined as $\mathbf{s}^{\Im}\left(\mathbf{x}^{\Im}\right)=\mathbf{u}^1\left(\mathbf{x}^{\Im}\right)-\mathbf{u}^2\left(\mathbf{x}^{\Im}\right)$.

At the point $\mathbf{x}^{\Im}$ a reference area is considered; at the micromechanical level, the reference area is split in the undamaged and damaged part.

The damage parameter $D^{\Im}$ is introduced as the ratio between the damaged area with respect to the reference area; it can vary from zero to one: $D^{\Im}=0$ corresponds to the undamaged state, while $D^{\Im}=1$ corresponds to the completely damaged state. The interface constitutive relationship is formulated:

$$\boldsymbol{\sigma}^{\Im}=\mathbf{K}^{\Im}\left[\mathbf{s}^{\Im}-D^{\Im}(\mathbf{c}^{\Im}+\mathbf{p}^{\Im})\right] \quad (11)$$

where $\mathbf{K}^{\Im}$ is the stiffness matrix, $\mathbf{c}^{\Im}$ is the unilateral contact vector and $\mathbf{p}^{\Im}$ is the sliding friction vector.

A local coordinate system on the interface $\left(x_N, x_{T1}, x_{T2}\right)$ is introduced; the subscripts $_N$, $_{T1}$ and $_{T2}$ indicate the normal and the two tangential directions to the interface, respectively. In this coordinate system, the stiffness matrix, the unilateral contact vector and the sliding friction vector are represented as:

$$\mathbf{K}^{\Im}=\begin{bmatrix} K_N & 0 \\ 0 & \mathbf{K}_T \end{bmatrix}$$
$$\mathbf{c}^{\Im}=H(s_N)\begin{Bmatrix} s_N \\ \mathbf{0} \end{Bmatrix} \qquad \mathbf{p}^{\Im}=\begin{Bmatrix} 0 \\ \mathbf{p}_T \end{Bmatrix} \quad (12)$$
$$\mathbf{K}_T=\begin{bmatrix} K_{T1} & 0 \\ 0 & K_{T2} \end{bmatrix} \quad \mathbf{p}_T=\begin{Bmatrix} p_{T1} \\ p_{T2} \end{Bmatrix}$$

In order to define the evolution of the inelastic slip $\mathbf{p}^{\Im}$, the stress, given by equation (11), is rewritten in the following form:

$$\boldsymbol{\sigma}^{\Im}=\boldsymbol{\sigma}_d^{\Im}+(1-D^{\Im})\mathbf{K}^{\Im}\left(\mathbf{c}^{\Im}+\mathbf{p}^{\Im}\right) \quad (13)$$

defining the contact-frictional stress $\boldsymbol{\sigma}_d^{\Im}$ as:

$$\boldsymbol{\sigma}_d^{\Im}=\mathbf{K}^{\Im}\left(\mathbf{s}^{\Im}-D^{\Im}\left(\mathbf{c}^{\Im}+\mathbf{p}^{\Im}\right)\right)=\begin{Bmatrix} \sigma_{dN} \\ \boldsymbol{\sigma}_{dT} \end{Bmatrix} \quad (14)$$

with $\boldsymbol{\sigma}_{dT}=\left\{\sigma_{dT1} \quad \sigma_{dT2}\right\}^T$.

It is assumed that the contact-frictional stress $\boldsymbol{\sigma}_d^{\Im}$ governs the evolution of the inelastic slip $\mathbf{p}^{\Im}$. In particular, the classical Coulomb yield function is introduced:

$$\begin{aligned}\phi\left(\boldsymbol{\sigma}_d^{\Im}\right)&=\mu\left\langle\sigma_{dN}\right\rangle_-+\left\|\boldsymbol{\sigma}_{dT}\right\|= \\ &=\mu\sigma_{dN}+\left\|\boldsymbol{\sigma}_{dT}\right\|\end{aligned} \quad (15)$$

where μ is the friction coefficient, the symbol $\langle\bullet\rangle_-$ denotes the negative part of number $\bullet$ and the symbol $\|\bullet\|$ indicates the norm of $\bullet$.

For the evolution of the components of the vector $\mathbf{p}^{\Im}$, the following non-associated flow rule is considered:

$$\dot{\mathbf{p}}^{\Im}=\dot{\lambda}\begin{Bmatrix} 0 \\ \dfrac{d\phi}{d\boldsymbol{\sigma}_{dT}} \end{Bmatrix}=\dot{\lambda}\begin{Bmatrix} 0 \\ \dfrac{\boldsymbol{\sigma}_{dT}}{\left\|\boldsymbol{\sigma}_{dT}\right\|} \end{Bmatrix} \quad (16)$$

The model is completed with the classical loading-unloading Khun-Tucker conditions, $\dot{\lambda}\geq 0, \quad \phi\leq 0, \quad \dot{\lambda}\phi=0$.

It can be remarked that the contact-frictional problem can be activated only when the interface damage is greater than zero.

About the evolution of the interface damage parameter $D^{\Im}$, a model which accounts for the coupling of normal and tangential modes of fracture, is considered. In fact, the three quantities η_N, η_{T1} and η_{T2}, defined as the ratios between the first cracking relative displacement s_N^0, s_{T1}^0 and s_{T2}^0 and the full damage relative displacement s_N^f, s_{T1}^f and s_{T2}^f, are introduced:

$$\begin{aligned}\eta_{T1}&=\frac{s_{T1}^0}{s_{T1}^f}=\frac{s_{T1}^0\sigma_{T1}^0}{2G_{cT1}} \\ \eta_{T2}&=\frac{s_{T2}^0}{s_{T2}^f}=\frac{s_{T2}^0\sigma_{T2}^0}{2G_{cT2}} \\ \eta_N&=\frac{s_N^0}{s_N^f}=\frac{s_N^0\sigma_N^0}{2G_{cN}}\end{aligned} \quad (17)$$

where σ_N^0, σ_{T1}^0 and σ_{T2}^0 are the peak stresses corresponding to the first cracking relative

displacement and G_{cN}, G_{cT1} and G_{cT2} are the specific fracture energies in normal and tangential modes, respectively. Then, the parameter η, which relates the modes of fracture, is defined as follows:

$$\eta = \frac{s_{T1}^{\ 2}}{\left\|\tilde{\mathbf{s}}\right\|^2}\eta_{T1} + \frac{s_{T2}^{\ 2}}{\left\|\tilde{\mathbf{s}}\right\|^2}\eta_{T2} + \frac{\left\langle s_N \right\rangle_+^2}{\left\|\tilde{\mathbf{s}}\right\|^2}\eta_N \tag{18}$$

where $\tilde{\mathbf{s}} = \left\{ \begin{array}{ccc} s_{T1} & s_{T2} & \left\langle s_N \right\rangle_+ \end{array} \right\}^T$. The relative displacement ratios are introduced as:

$$Y = \sqrt{Y_N^2 + Y_{T1}^2 + Y_{T2}^2} \tag{19}$$

with

$$Y_N = \frac{\left\langle s_N \right\rangle_+}{s_N^0} \quad Y_{T1} = \frac{s_{T1}}{s_{T1}^0} \quad Y_{T2} = \frac{s_{T2}}{s_{T2}^0} \tag{20}$$

Finally, the damage parameter is assumed to be a function of the history of the relative displacement as follows:

$$D^{\mathfrak{I}} = \max_{history}\left\{0, \min\left\{1, \tilde{D}^{\mathfrak{I}}\right\}\right\} \tag{21}$$

with

$$\tilde{D}^{\mathfrak{I}} = \frac{Y-1}{Y\left(1-\eta\right)} \tag{22}$$

2.3 Interface damage model with coupling

A coupled interface model, obtained considering different ways of coupling the body and the interface damage, is proposed. In the first case the coupling approach assumes that the interface damage is the highest value between the interface damage and the body damage evaluated on the adhesion surface [7]:

$$D^I\left(\mathbf{x}\right) = \max\left\{D^{\mathfrak{I}}\left(\mathbf{x}\right), D_t^{\Omega}\left(\mathbf{x}\right)\right\} \tag{23}$$

with $D^I\left(\mathbf{x}\right)$ the coupled interface damage evaluated at a point $\mathbf{x}$ of the interface.

In the second case, when the body damage occurs, a representative area A of the interface is assumed to be decomposed in two parts A^W and $A^{\mathfrak{I}}$. In fact, the damaging of the support induces the presence of a microfracture in the third layer of the interface made of cohesive support material, characterized by a corresponding area $A^W = D_t^{\Omega} A$. Because of the presence of the microcrack, the stress $\boldsymbol{\sigma}^W$ in A^W is equal to zero if the microcrack is open and it is different from zero when it is closed. In the remaining part of the representative area $A^{\mathfrak{I}} = \left(1 - D_t^{\Omega}\right) A$, it is assumed that the mechanical response is governed by the constitutive model described by equation (11). Thus, the overall constitutive response of the coupled interface is obtained as:

$$\boldsymbol{\sigma}^I = D_t^{\Omega}\boldsymbol{\sigma}^W + \left(1 - D_t^{\Omega}\right)\boldsymbol{\sigma}^{\mathfrak{I}} \tag{24}$$

with $\boldsymbol{\sigma}^{\mathfrak{I}}$ given by equation (11) and $\boldsymbol{\sigma}^W = \left\{ \begin{array}{ccc} K_N\left(s_N - c_N\right) & 0 & 0 \end{array} \right\}^T$, where c_N is the normal component of $\mathbf{c}^{\mathfrak{I}}$.

3 NUMERICAL APPLICATIONS

Numerical procedures for solving the equations governing the nonlinear response of the composite structural system, are developed.

A step by step time integration algorithm is adopted in order to solve the evolutive equations of the proposed body-interface detachment model. In particular, the time integration is performed adopting a backward-Euler implicit procedure. The proposed numerical procedure is implemented in the finite element code FEAP [11].

Some numerical applications are carried out in order to assess the ability of the proposed model in describing the detachment phenomenon of the FRP strengthening from the cohesive material.

In particular, in the following applications Model 1 indicates the interface model, in which the coupling is taken into account assuring that the interface damage is the highest value between the interface damage and the body damage evaluated on the bond surface, while Model 2 indicates the formulation developed on the basis of the discussed simplified micromechanical analysis.

3.1 Tensile test

The geometry and loading conditions of the scheme considered to perform the tensile test are shown in Figure 1. The geometrical parameters are $b = 500$ mm , $h = 49$ mm and an unit thickness is considered. The material properties adopted are: $E_1 = 15300$ MPa , $\nu_1 = 0.2$, $E_2 = 160000$ MPa , $\nu_2 = 0.3$, $K_N = K_T = 600$ N/mm^3, $\mu = 0.5$, $\sigma_N^0 = \sigma_T^0 = 4.7$ MPa , $G_{cN} = G_{cT} = 0.34$ N/mm,

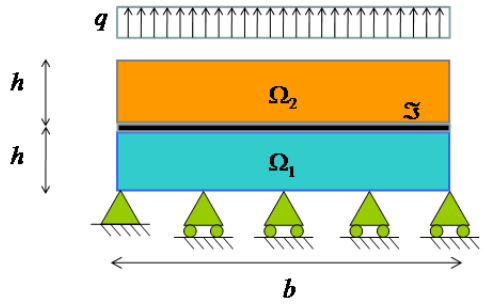

Figure 1: Scheme of the uniaxial test.

where E_1, ν_1, E_2 and ν_2 are the Young modulus and the Poisson coefficient of the body Ω_1 and Ω_2, respectively.

Two dimensional plane strain four node quadrilateral elements are adopted to model the bodies Ω_1 and Ω_2 and four node interface elements are used to model the interface $\Im$.
In order to investigate the influence of the damaging behavior of the body Ω_1 on the tensile response of the interface and, as a consequence, of the whole structure, three analyses are developed considering different values of the damage strain threshold ε_0 and keeping constant the fracture energy G_c for the body Ω_1; in particular it is set: $\varepsilon_0 = 0.00016$ for the Case 1; $\varepsilon_0 = 0.00026$ for the Case 2; $\varepsilon_0 = 0.00036$ for the Case 3. In each case the nonlocal radius is set $R = 15$ mm . The three analyses are performed considering as interface model the two coupled damage approaches previously presented (Model 1 and Model 2).

In Figure 2 and Figure 3, the numerical response obtained adopting the Model 1 and the Model 2 are shown, respectively. In these figures, the results are plotted with a dotted line for Case 1, with a dashed line for the Case 2 and with a solid line for the Case 3. Computations are performed adopting an arc-length technique and considering the relative normal displacement s_N at the interface as control parameter.

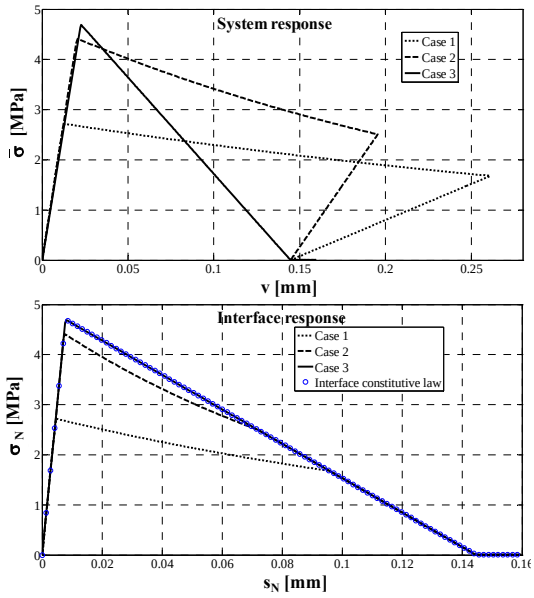

Figure 2: Numerical results of the uniaxial test adopting the Model 1: overall response and interface behavior .

With reference to Figure 2, it can be noted that in the Case 3 the mechanical response of the structure is strongly influenced by the softening behavior of the interface as in this analysis the damage does not occur in the body and the tensile interface response is equal to the interface constitutive law. In the other two cases, the tensile mechanical response of the structure depends on the coupling of the body and interface damage. In fact, after the achievement of the peak stress, which coincides with the tensile strength of the body, the softening branch depends on the evolution of the damage in the body until the interface damage, governed by the relative displacement, becomes higher than the body one at the interface. At this point of the analysis the softening tensile response is due

to the development of the interface damage governed by the relative displacement.

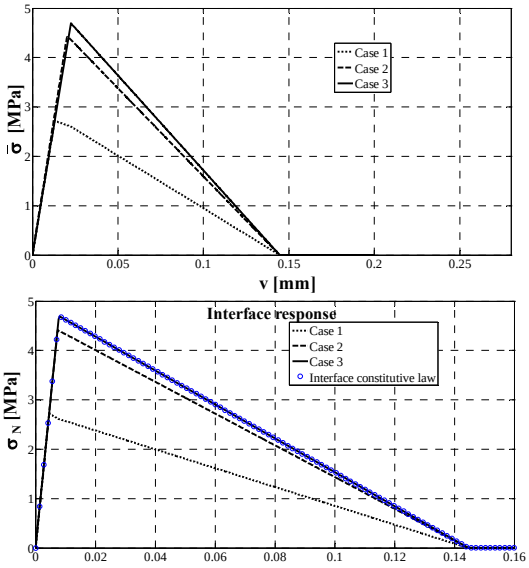

Figure 3: Numerical results of the uniaxial test adopting the Model 2: overall response and interface behavior.

From Figure 2 and Figure 3, it appears evident that in the Case 3 the analyses, performed adopting the two proposed coupled interface formulations lead to the same numerical results. On the contrary, in the Case 1 and 2 the softening response, obtained adopting the Model 1 and 2, presents some significant differences. In fact, the results carried out adopting the Model 1 show that the softening behavior is strongly influenced by the evolution of the body damage until the interface damage becomes higher than the body one. From this point of the analysis, the body damage does not increase anymore and the softening behavior is only governed by the evolution of the interface damage. On the other hand, in the results obtained considering the Model 2, the softening behavior is strongly influenced by the body damage during the whole detachment process, also when the interface damage becomes to develop and the body damage does not evolve anymore. Thus, the degradation process results faster for the Model 2 than for the Model 1.

3.2 Comparison with experimental data

The two coupling approaches, Model 1 and Model 2, are tested throught a comparison with experimental data regarding detachment tests of CFRP (Carbon Fiber Reinforced Polymer) laminates externally applied on ancient clay bricks [12].

The geometry and the boundary conditions adopted in the detachment tests is illustrated in Figure 4. The CFRP laminate, with a nominal width $b_f = 36\text{mm}$ and thickness of 0.22 mm, is glued on a clay brick of size 245x143x61 mm^3.

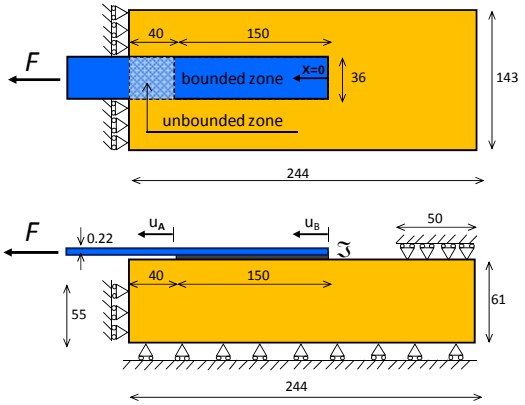

Figure 4: Detachment test: boundary conditions and geometry, (units in mm).

The mechanical properties of the materials, set on the basis of tests performed during the experimental campaign [12] and assumed in the numerical analyses are the following:

-Clay-brick:

$$E_m = 8300\ \text{MPa} \qquad \nu_m = 0.13$$
$$R = 6\,\text{mm}$$
$$\varepsilon_0 = 0.00023 \qquad G_c = 0.001\ \text{N/mm}^2$$
$$\kappa_u = -0.06 \qquad \sigma_y = -12.3\ \text{MPa}$$

-CFRP-laminate:

$$E_{FRP} = 230000\ \text{MPa} \quad \nu_{FRP} = 0.3$$

- interface:

$$K_{T1} = K_{T2} = 370\ \text{N/mm}^3$$
$$\mu = 0.5$$
$$\sigma_N^0 = \sigma_T^0 = 7\ \text{MPa}$$
$$G_N = G_T = 0.7\ \text{N/mm}$$

Four different numerical analyses are developed. In particular, it is considered: a linear elastic support; a support characterized by damaging behavior and the uncoupled model for the interface; a support characterized by damaging behavior and Model 1 as coupling approach; a support characterized by damaging behavior and Model 2 as coupling approach.

The numerical computations are performed with the arc-length technique assuming as control parameter the horizontal displacement u_B at the unloaded end.

The numerical and experimental results are reported in Figure 5. They are plotted in term of the ratio of adhesion force to nominal width of CFRP, F/b_f, versus the horizontal displacement, u_A, of CFRP strips. From the comparison of Figure 5, it can be emphasized that Model 2, compared to the other models, better captures the maximum decohesion force and sightly tends to underestimate the ductility of the mechanical system.

The numerical results obtained with the coupled theory are more stable and lead to a faster convergence with respect to one provided by the uncoupled model.

Futhermore, an experimental and numerical comparison of the CFRP laminate strains along the bounded zone in correspondece of five equilibrium states is performed and illustrated in Figure 6. By observing the figure it is evident that Model 2 is able to catch the CFRP strengthing strains more accurately than the ones obtained with the Model 1.

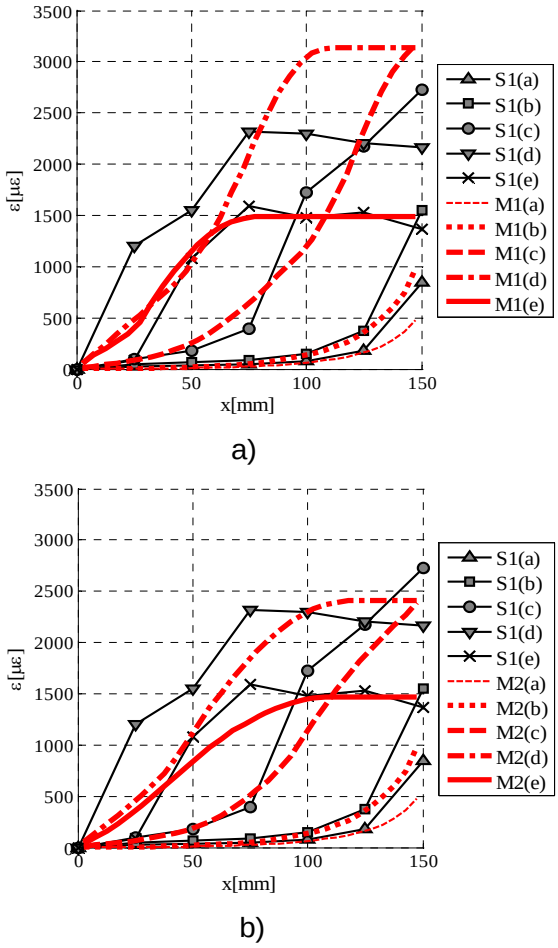

Figure 6: CFRP laminate strains: a) experimental and numerical comparison adopting Model 1; b) experimental and numerical comparison adopting Model 2.

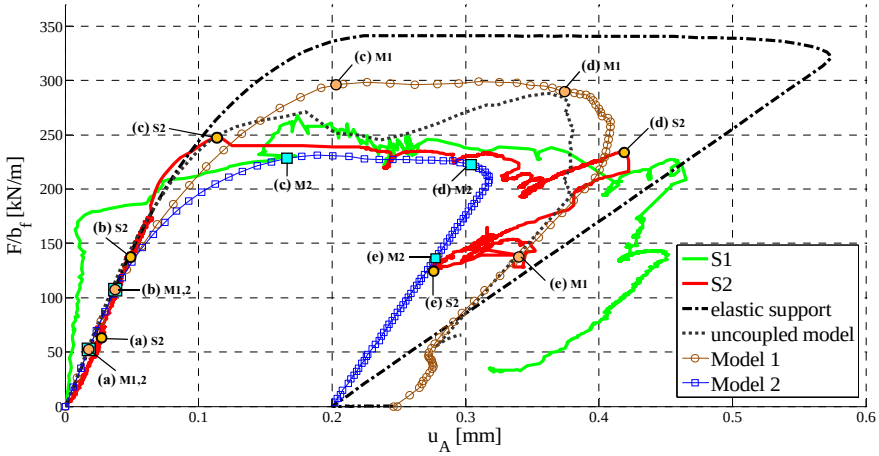

Figure 5: Comparison between experimental and numerical results.

3.3 Analysis of a FRP strengthened panel

The influence of the FRP strengthening on the global behavior of a masonry panel, adopting the proposed FRP-masonry interface model, is studied. The wall, as schematically represented in Figure 7, is characterized by dimensions 1200x2400 mm^2 and thickness 500 mm. A constant uniformly distributed vertical load $q = 30\,\mathrm{kN/m}$ and a monotonically increasing distributed horizontal load, whose resultant is denoted with F, are applied on the top of the panel.

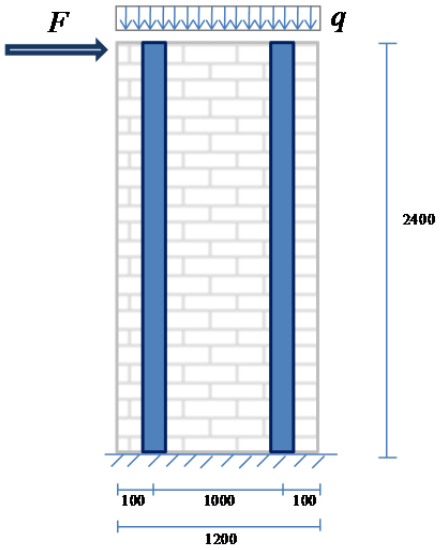

Figure 7: Geometry of the FRP-strengthened panel (units in mm).

Initially, the mechanical response of the un-strengthened panel is analyzed; then, the wall is reinforced applying two FRP strips of thickness 0.17 mm and a width 100 mm on both the two panel surfaces according to the arrangement shown in Figure 7. The mechanical properties adopted in the analyses are the following:

-masonry:

$$E_m = 1000\ \mathrm{MPa} \qquad \nu_m = 0.1$$
$$R = 150\,\mathrm{mm}$$
$$\varepsilon_0 = 0.0002 \qquad G_c = 0.0095\ \mathrm{N/mm^2}$$
$$\kappa_u = -0.06 \qquad \sigma_y = -20\ \mathrm{MPa}$$

-FRP-strips:

$$E_{FRP} = 230000\ \mathrm{MPa} \qquad \nu_{FRP} = 0.3$$

- interface:

$$K_{T1} = K_{T2} = 310\ \mathrm{N/mm^3}$$
$$\mu = 0.5$$
$$\sigma^0_{T1} = \sigma^0_{T2} = 6\ \mathrm{MPa}$$
$$G_{cT1} = G_{cT2} = 0.3\ \mathrm{N/mm}$$

In particular, two dimensional plane strain four node quadrilateral elements are adopted to model the masonry panel and two node truss elements are used to model the FRP-strengthening and four node interface elements to model the masonry-FRP interface.

In the case of the reinforced wall four analyses are performed assuming the following FRP-masonry interface models: the Model 1, the Model 2, the uncoupled model and a perfect adhesion model.

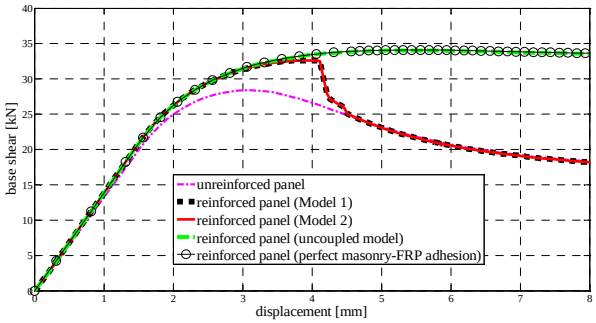

Figure 8: Base shear vs. top displacement curves.

The results of the computations are reported in Figure 8 in term of base shear versus top displacement curves. From the figure is possible to observe that: the reinforced panel models are able to simulate the increase of shear strength and initial stiffness due to presence of FRP-strengthening; the Model 1 and the Model 2 lead to the same numerical response as the interface damage governed by relative displacement does not occur; assuming the two coupled interface damage approaches, the value of the peak load results lower than the one obtained considering the uncoupled model as the damage developed in the masonry influences also the degradation state of the FRP-masonry interface; the coupled damage formulations accelerate the

softening behavior of the wall compared to one obtained assuming the uncoupled model; adopting the uncoupled damage theory for the FRP-masonry interface, the nonlinear behavior of the wall results equal to the one in which the perfect adhesion is ensured.

4 CONCLUSIONS

Two different ways of coupling the body and the interface damage are presented. A tensile test is performed in order to emphasize some significant differences of the two proposed coupled formulations. Numerical simulations concerning detachemnt tests show the capacity of the coupling approach, based on micromechanical assumptions, in reproducing more accurately the experimental behavior, specially in terms of peak load and CFRP laminate strains. Finally, numerical analyses of the FRP-strengthened wall demonstrates that the coupled damage theory, taking into account that the masonry damage influences the degradation process of the FRP-masonry interface, leads, compared to the uncoupled theory, to a decrease of the bearing capacity and an acceleration of the overall softening behavior.

REFERENCES

[1] Plevris, N., Triantaffilou, T.C. and Veneziano, D., 1995. Reliability of RC members strengthened with CFRP laminates, *Journal of Structural Engineering ASCE*, **121**: 1037-1044.

[2] Triantafillou, T.C. and Fardis, M.N., 1997. Strengthening of historic masonry structures with composite materials, *Materials and Structures*, **30**: 486-496.

[3] Galati, N., Tumialan, G. and Nanni, A., 2006. Strengthening with FRP Bars of URM Walls Subject to Out-of- Plane Loads, *Construction and Building Materials*, **20-21**: 101-10.

[4] Ferracuti, B., Savoia, M. and Mazzotti, C., 2006. A numerical model for FRP-concrete delamination, *Composites Part B: Engineering*, **37**: 356-364.

[5] Grande, E., Milani, G. and Sacco, E., 2008. Modelling and analysis of FRP-strengthened masonry panels, *Engineering Structures*, **30**: 1842-1860.

[6] Freddi, F. and Fremond, M., 2006, Damage in domains and interfaces: a coupled predictive theory, *Journal of Mechanics of Materials and Structures*, **1**: 1205-1233.

[7] Marfia, S., Sacco, E. and Toti, J., 2012. A coupled interface-body nonlocal damage model for FRP strengthening detachment, *Computational Mechanics*, 50 (3): 335-351.

[8] Mazars J. and Pijaudier-Cabot G., 1989. Continuum damage theory: application to concrete, *Journal of Engineering Mechanics ASCE*, **115**: 345-365.

[9] Alfano, G. and Sacco E., 2006. Combining interface damage and fiction in a cohesive-zone model, *International Journal For Numerical Methods in Engineering*, **68**: 542-582.

[10] Sacco, E. and Toti, J., 2010. Interface elements for the analysis of masonry structures, *International Journal for Computational Methods in Engineering Science and Mechanics*, **11**: 354-373.

[11] Taylor, R.L., 2008. FEAP - A Finite Element Analysis Program, Ver. 8.2 User Manual, Department of Civil & Environmental Engineering, University of California, Berkeley, www.ce.berkeley.edu/feap.

[12] Carrara, P., Ferretti, D. and Freddi F., 2012, Debonding behavior of ancient masonry element strengthened with FRP, *Composites Part B: Engineering*, in press, DOI:http://dx.doi.org/10.1016/j.compositesb.2012.04.029.